Polymer(Korea). Published by the Polymer Society of Korea
Vol. 12, No. 3, 1988

상반전법에 의한 비대칭막의 생성기구

강 용 수 · 김 효 진* · 김 영 하 · 조 원 호*
한국과학기술원 고분자화학연구실 · *서울대학교 섬유공학과
(1988년 4월 7일 접수)

The Mechanism of Asymmetric Membrane Formation via Phase Inversion Process

Yong-Soo Kang, Hyo-Jin Kim, *Young-Ha Kim, and Won-Ho Jo
Polymer Chemistry Lab., KAIST P.O.Box 131 Cheongryang, Seoul 131-650, Korea
**Department of Textile Engineering, Seoul National University, Seoul 151-742, Korea*
(Received April 7, 1988)

요 약 : 상반전 과정을 통해 비대칭막의 생성기구를 조사하고, 열역학적 및 동력학적 영향을 살펴보았다. 폴리술폰의 용해도 계수지도를 얻고 이로 부터 용매(NMP), 비용매(ethanol) 그리고 용매첨가제(FA : 포름산)를 선택했으며 구름점 측정으로부터 상분리도를 작성했다. 용매속의 FA 함량이 증가함에 따라 용액의 열역학적 안정도가 감소했다. 폴리술폰 비대칭막을 만들어 표면 및 단면구조를 SEM 으로 관찰했으며, 산소투과도를 측정했다. 상반전 과정에서의 비용매의 투과속도를 측정하였으며, 투과속도가 클 때 스폰지형 막을 만들 수 있었는데 이는 이때까지의 결과와 다른 새로운 발견이었다. 막에서의 대공형성 기구도 상반전 과정을 현미경으로 관찰하였으며 용액의 점도 및 표면장력과의 연관성을 검토했다.

Abstract : Thermodynamic and kinetic aspects of phase inversion process were investigated to elucidate the mechanism of asymmetric membrane formation. A solubility parameter map of polysulfone was obtained. A solvent (NMP), a solvent additive (FA : formic acid) and a non-solvent(ethanol) were chosen on the basis of the solubility parameter map. A series of cloud points measurement resulted in a phase diagram illustrating that the polymer solution is thermodynamically unstable with increasing amount of FA in the solvent mixture. An asymmetric mermbrane prepared was characterized in terms of the skin structure and the cross-sectional morphology as well as the oxygen permeability. The diffusion coefficients of non-solvent into polymer solutions from the precipitation kinetics were also obtained. The sponge-like membrane was prepared with the system of the rapid exchange rate of non-solvent and solvent. This observation is contradictory to common observations. The macrovoids formation was also investigated by an optical microscope and seemed to be attributable to the non-solvent intrusion through the surface microcracks at the surface, which, in turn, related to the viscosity and surface tension of polymer solution.

INTRODUCTION

The maiorty of synthetic asymmetric membrasnes are produced by the phase inversion process. This process involves the inversion of liquid homogeneous polymer solution into a two-phase system with a solid, polymer-rich phase forming the rigid membrane structure and a liquid, polymer-lean phase forming membrane pores. The phase inversion process dictates the morphology of final membrane, which, in turn, governs the characteristic transport properties of the membrane such as flux and selectivity or rejection in gas separation, reverse osmosis and ultrafiltration process. The skin (the uppermost surface) structure and cross-sectional morphology of the asymmetric membranes strongly depend upon the thermodynamics and kinetics for the phase inversion process.[1~5]

A phase diagram and a solubility parameter map normally give us some information on thermodynamic properties of the polymer solution.[6~11] Although the thermodynamic description predicts the overall porosity of final membranes, it does not give us any information on pore size and its distribution of the membrannes.[1] Therefore, the pore size and its distribution of membrane cross-section should be affected by the kinetic effect, particularly, the exchange rate of solvent and non-solvent at the interphase of polymer solution and gelation medium. According to Strathmann, when the exchange rate is slow, the skin pores are large and the membrane cross-section is more-like sponge type.[1] On the other hand, when the exchange rate is fast, the skin is less porous and the cross-section is finger-like.[1] This behavior is generally accepted to be common in phase inversion membranes. Recently, some mathematical models have been developed to describe the mass transport behavior during the phase inversion process.[12,13] However, the mechanism of asymmetric membrane formation via phase inversion process has not been understood well yet. The better understanding of the mechanism certainly helps to tailor and produce the membrane morphology needed.

In this study, in order to understand the mechanism of asymmetric membrane formation process, we examined the effect of the thermodynamic and kinetic properties of polymer solution system, particularly the effect of the thermodynamic stability and the solvent exchange rate on the membrane morphology. The morphology of the membrane was characterized by SEM photographs and oxygen permeability. The macrovoid formation mechanism in the membrane was also investigated through an optical microscope and was interpreted in terms of the viscosity and surface tension of the polymer solution.

EXPERIMENTAL

Materials : Polysulfone (PSf) is Udel-1700 of Union Cabide, amorphous and has M.W.=30,000.

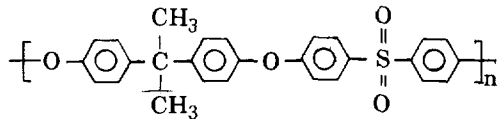

NMP (1-Methyl-2-pyrrolidinone), formic acid (FA), ethanol and PSf were used without further purification.

Solubility and Phase Diagram of PSf: PSf(1 g) was added into various kinds of solvents(9 g) and kept at 25 ℃ for 24 hours. Dissolving behavior was observed visually to classify a good solvent, a swelling agent and a non-solvent. In order to obtain a phase diagram, a PSf solution was placed in a test tube at 25 ℃. The non-solvent (ethanol) is slowly added to this solution until the clear polymer solution becomes turbid visually. The point where the solution becomes turbid is referred to as the cloud point. The solution composition at the cloud point was computed from the amount of polymer, solvent and non-solvent present in the test tube. A phase diagram was obtained from a series of the cloud points observed.

Membrane Preparation and Characterization : PSf solution was prepared and cast on a glass plate at ambient temperature. The compositions of the polymer solutions are listed in Table 1. The thickness of cast solution was controlled with a Doctors kinfe. The polymer solution cast on a glass plate

Table 1. Sample Compositions of Polymer Solutions.

Code	PSf[a](g)	NMP[b](g)	FA[c](g)
N	20	80	0
F4	20	76	4
F8	20	72	8
F12	20	68	12

[a] polysulfone,
[b] N-methyl pyrrolidinone,
[c] formic acid

was, then, immersed immediately into the gelation medium of ethanol at 25 ℃ and kept there for 24 hours. The membrane was then removed and dried at room temperature. The skin and cross-sectional morphology were characterized by SEM (scanning eletron microscope) with a Hitachi scanning electron microscope(Model S-510, Tokyo, Japan). For measuring the permeation properties, a membrane of 1.7 cm in diameter was placed in a conventional gas permeation cell, the upstream pressure was kept at 5 atm during the experiment and the downstream side was open to atmosphere. The oxygen flux at steady state was measured with a soap bubble flow meter.

Precipitation Kinetics : A drop of casting solution was placed between two optical slide glasses and a drop of ethanol was introduced near the edge of the ploymer solution. Then, as ethanol diffuses into between two slide glasses the precipitation starts to occur and the precipitation front moves inward the center of polymer soluton. These phenomena were observed under an optical microscope (x 80) and photographs were taken with time. The traveling distance of the precipitation front were measured from the optical photographs.

Viscosity and Surface Tension of Polymer Solution : The viscosity of polymer solution(20% by weigt) was measured by Haake torsional viscometer (Haake RV2, Karlsruhe, FRG) with different shear rate at 25 ℃. The zero shear viscosity was calculated from the data of viscosity and shear rate by extrapolating to zero-shear rate.

The surface tension was measured by the Wilhelmy plate meathod using the Electrobalance RTL of Wet-Tek (Biomaterials International Co., Utah, U. S. A.)

RESULTS AND DISCUSSION

Solution Characteristics

Fig. 1 is the solubilty parameter map of PSf. A solvent is classified into a good solvent, swelling agent or non-solvent based on the solubilizing power for polymer, which was plotted in terms of the Hansen solubility parameters. The region enclosed by the circle in Fig. 1 represents good solvent. Swelling agent and non-solvent are on the border and outside of the circle, respectively. On the basis of the solubility paramter map the solvent (NMP) and non-solvent (ethanol) were chosen, and FA is employed as a solvent additive and mixed with NMP for a mixed solvent to

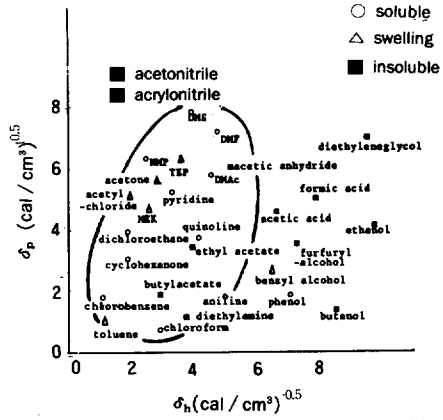

Fig. 1. Solubility parameter map of polysulfone.

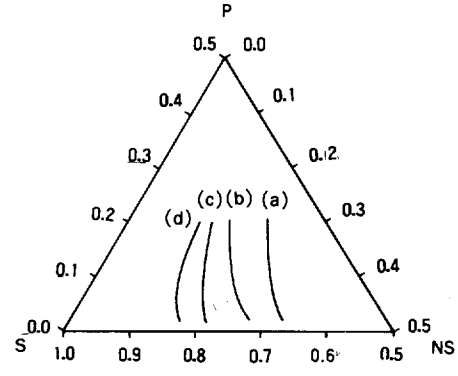

Fig. 2. Ternary phase diagram of polysulfone solution (a) N, (b) F4, (c) F8, (d) F12 : P ; polymer, S ; solvent and NS ; non-solvent.

control the solubilizing power of NMP.

A semes of the cloud points measurement results in the ternary phase diagram as shown in Fig. 2. The solid lines in Fig. 2 represent the liquid-liquid phase boundary (called the binodal), where the homogeneous liquid solution starts to demix into two liquid phases. Every composition outside the binodal is miscible, while one inside the binodal demixes into polymer-rich phase and the polymer-poor phase. Fig. 2 illustrates that the binodal curve shifts to left as the amount of FA, a non-solvent, in the mixed solvent increases. This indicates that the polymer solution becomes thermodynamically unstable and readily separates into two phases when the fraction of FA in the mixed solvent is large. Thus, the sample F12, for instance, is thought to be partially desolvated and thermodynamically unstable. In other words, the system is very intolerable to the non-solvent. In this situation, the small concentration fluctuation, e. g., the introduction of the small amount of non-solvent into the polymer solution, causes to generate stable nuclei and phase separation starts. On the other hand, when PSf is dissolved in a good solvent, for instance the sample N, the system is thermodynamically stable and the polymer chains interact strongly with solvent molecules. Thus, the introduction of non-solvent can not readily cause the system to start demixing, and the binodal curve, consequently, shifts to right of the phase of the diagrm as shown in Fig. 2.

Membrane morphology

As shown in Fig. 3 (a), the large pores (approxmately 0.2-0.3 μm in diameter) on the skin were observed

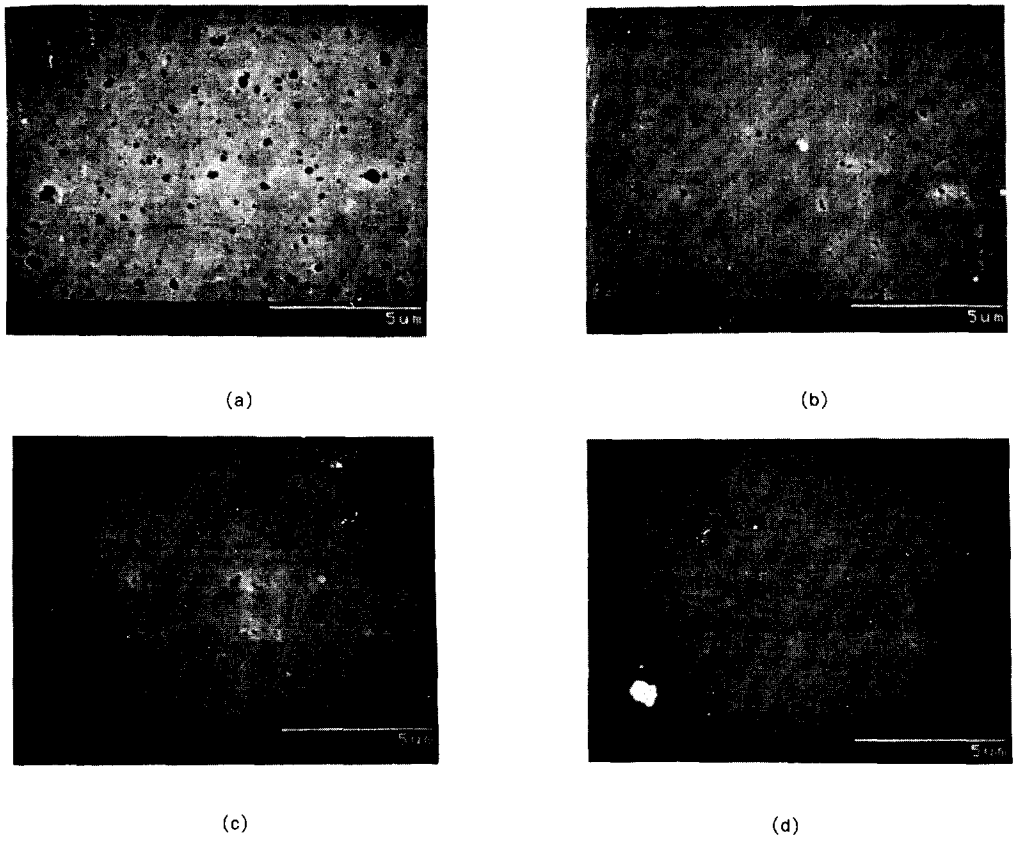

Fig. 3. SEM micrographs of membrane skins (x 8000). (a) N, (b) F4, (c) F8 and (d) F12.

for the membrane N. The size of pores on the skin decreases as the amount of FA in the mixed solvent increases. For the case of F12, where the highest amount of FA is contained, the skin is very smooth, clean and pore-free under this magnifcation (Fig. 3(d)). Right after immersion of polymer solution into a gelation medium, solvent of the polymer solution diffuses out and the relatively small amount of non-solvent diffuses into the polymer solution. At this moment, if the polymer solution is thermodynamically stable, there is enough time to occur the nucleation and growth, which yields rather porous skin structure[11]. While, if solution is thermodynamically unstable, the very little concentration fluctuation causes the polymer solution to be separated into two phases. In this case, thus, there is not enough time to take place the nucleation and growth, but the instantaneous spinodal decomposition seems to take place, resulting in apparently smooth, pore-free surface under the limited magnification. In

Table 2. Properties of Polymer Solution and Membrane.[a]

Code	$D^{x}10^{5}$ (cm^2 / sec)	μ (mPa sec)	γ (dyne / sec)	$P^{x}10^{-3}$ (Barrer)[b]
N	1.66	1287.4	47.80	1.02
F4	1.85	1567.5	50.62	1.10
F8	2.87	2367.5	54.00	3.11
F12	3.62	3198.5	60.18	6.80

a : D : diffusion coefficient of ethanol,
μ : zero-shear viscosity of polymer solution,
γ : surface tension of polymer solution,
P : oxygen permeation coefficient.
b : Barrer=cm^3 / cm sec cmHg$\times 10^{-10}$

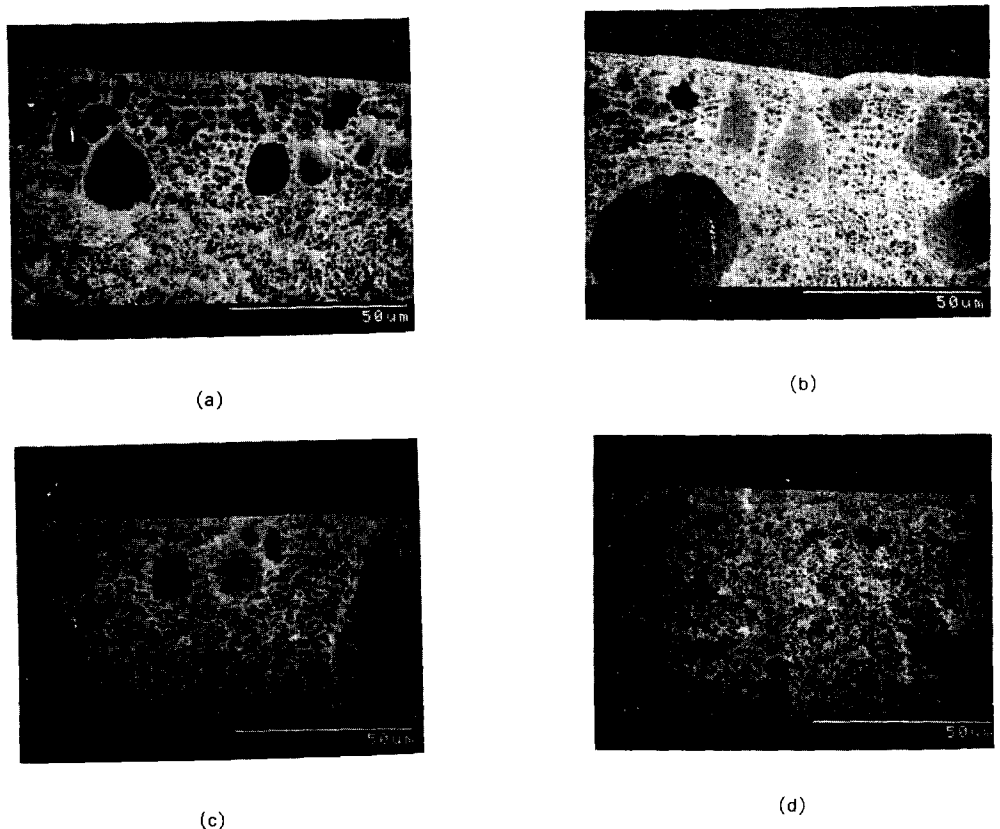

Fig. 4. SEM micrographs of membrane cross-sections (x 1000). (a) N, (b) F4, (c) F8 and (d) F12.

other words, the orignally highly entangled polymer chains at interphase are forzen at the moment when the non-solvent starts to diffuse into the polymer solution. Although the surface micrograph of the sample F12 does not show any pores as is in Fig. 3 (d), the sample F12 has the highest oxygen permeability as shown in Table 2, seemingly attributable to a tremendous number of the forzen intersegmental corridors for gas diffusion.

The cross-sectional morphology is also of importance to govern the transport properties of membrane. An important feature in the cross-sectional morpholgy is the presence of the macrovoids (few microns in diamter).Fig. 4 is the result of SEM micrographs taken from the cross-section of the membrane prepared. There are many macrovoids for the

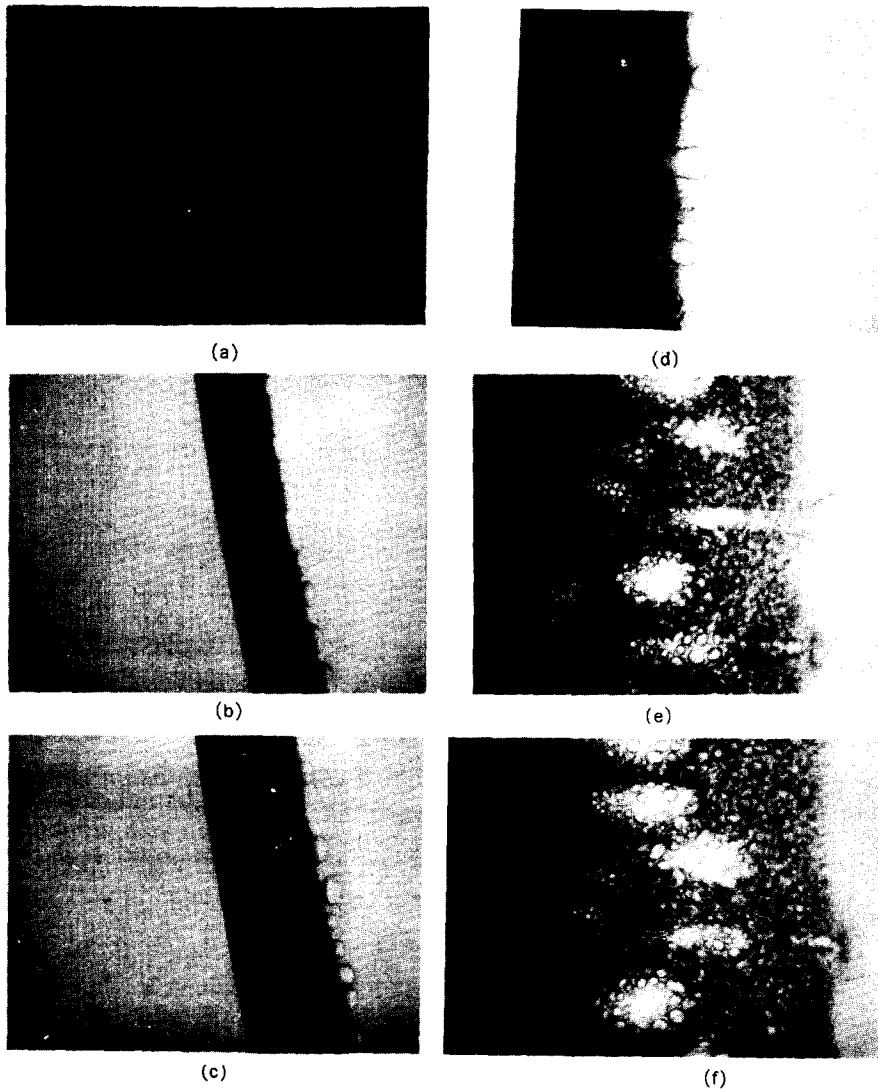

Fig. 5. Optical micrographs illustrating the nonsolvent intrusion (white bubble) through the precipitated region (black). The elapsed times are (a) 20 sec, (b) 1 min, (c) 2 min, (d) 6 min, (e) 21 min and (f) 26 min.

sample N, F4 and F8, but not the F12. According to the optical micrographs taken at different times (Fig. 5), the non-solvent appears to intrude into the polymer solution phase through the surface microcraks, which seem to be generated due to the microscopic surface roughness and mechanical

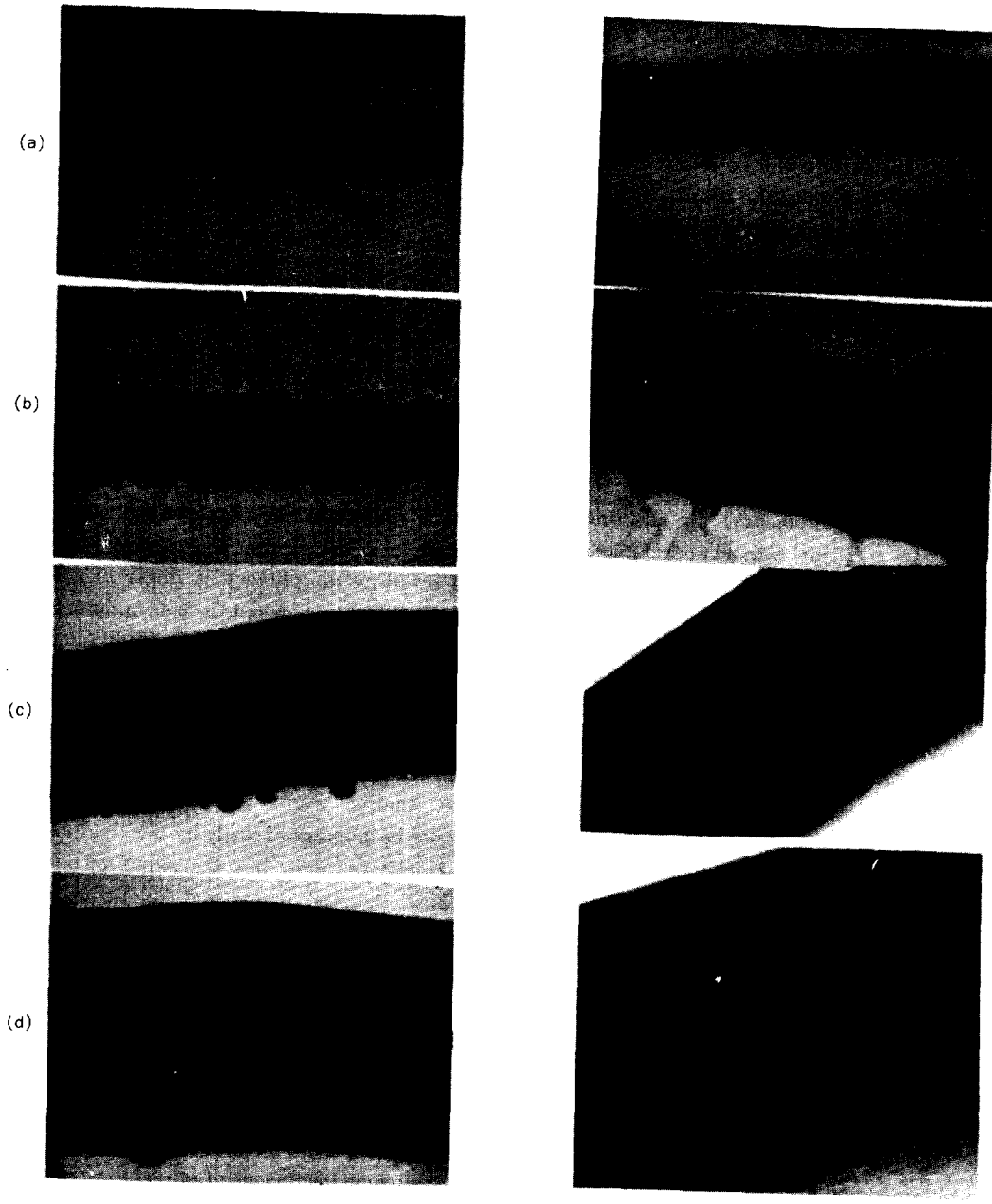

Fig. 6. Optical micrographs for precipitation kinetics of the samples N and F12. The elapsed times are (a) 10 sec, (b) 20 sec, (c) 100 sec and (d) 300 sec.

weakness at the moment when a polymer solution contacts with non-solvent. Interestingly, the non-solvent bubbles in Fig. 5 are always ahead of the precipitation front. In order to characterize the surface roughness and mechanical weakness indirectly, the viscosity and surface tension of the polymer solution were measured. When a solution has high viscosity and surface tension, it seems that the surface will be relatively smooth and strong, and therefore, the possibility of crack generation will be less and a macrovoid-free membrane can be obtained. As you can see in Table 2, the viscosity and surface tension increase with the amount of FA in the mixed solvent. Consequently, the surface of the sample F12, for instance, will be microscopically smooth and mechanically strong, and the number of macrovoids is reduced as shown in Fig. 4.

In order to investigate the effect of kinetic features on the membrane morphology, we measured the penetration rate of ethanol with an optical microscope in a model system, in which the polymer solution is placed between two slide glasses followed by the introduction of ethanol. The solution compositions are the same as Table 1. This model system was designed in order to lengthen the penetration time and path. The penetration distance was calculated with time from the optical micrographs as shown in Fig. 6. A plot of the penetration distance vs the square root of time was made in Fig. 7. The diffusion coefficients (D) of ethanol were calculated by following the equation derived by Strathman et. al.[15] and listed in Table 2.

$$x^2 = \frac{4D\varepsilon}{\tau}\ \frac{1-C_e}{1+C_e}t$$

where x and t are the penetration distance and time, respectively. C_e is the concentration of ethanol in the liquid phase at the point of precipitation, and is obtained for each sample from the phase diagram. The porosity (ε) and the tortuosity fator (τ) are assumed to be 0.5 and 2, respectively. From Table 2 and Fig. 4, it is concluded that, when the diffusion corefficient is high the membrane

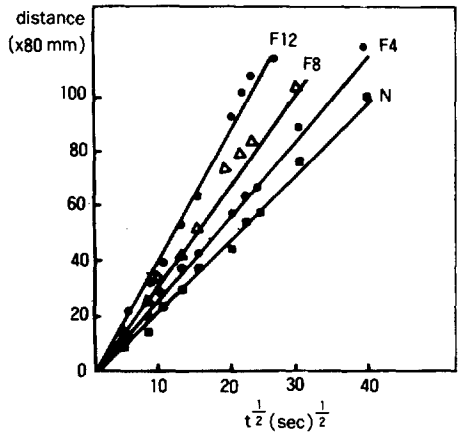

Fig. 7 A plot of the penetration distance of non-solvent (x) vs t with the different amount of FA in the solvent mixture.

has less macrovoids and become sponge-like structure, and when the diffusion coefficient is low the membrane has rather finger-like structure. However, Strathmann demonstrated from a polyamide-NMP system that when the penetration rate is fast, the resulting morphology is finger-like, and vice versa[1]. Thus, our result is contradictory to the common observations of the finger-like membrane with a system, where non-solvent penetration is fast. Therefore, it is implausible to conclude that the finger-like structure is obtained only from the system of high non-solvent penetration rate. Another words, the membrane morphology can not be determined solely by the thermodynamic or kinetic features, but the simultaneous effects of both thermodynamic and kinetic features are working in the membrane formation precess.

CONCLUSIONS

A polysulfone membrane prepared with the large amount of FA(a non-solvent) in a mixed solvent of NMP/FA has a smooth, pore-free skin structure as wee as a macrovoid-free cross-section. The diffusion coefficient of ethanol in the polymer solution increases with the amount of FA in the mixed solvent. However, it has been frequently reported that the sponge-like membrane was produced from a system of the solw exchange rate of solvent

and non-solvent in many literatures. Thus, this result is contradictory to common observations in the phase inversion membrane process. It is concluded from our experimental results that the skinless, macrovoids-free and highly permeable membrane can be also prepared when a polymer solution is thermodynamically unstable and when the exchange rate of solvent and non-solvent is high at the interphase between the polymer solution and gelation medium. The optical micrographs taken from the model system demonstrate that the macrovoid formation seems to be attributable to the intrusion of non-solvent through the microcracks generated on the interphase at the moment, when polymer solution initially contacts with non-solvent.

REFERENCES

1. H. Strathman, "Materials Science of Synthetic Membranes", Chap.8, D. R. Lloyd Ed. ACS Symp. 269, Washinton, D. C. 1985.
2. R. E. Kesting, " Materials Science of Synthetic Membranes", Chap.7, D. R. Lloyd Ed. ACS Symp. 269, Washinton, D. C. 1985.
3. L. Broens, D. M. Koenhen,and C. A. Smolders, *Desalination*, **22**, 205(1977).
4. L. Broens, F. W. Altena, C. A. Smolders, and D. M. Koenhen, *Desalination*, **32**, 33(1980).
5. M. A. Frommer and R. M. Messalem, *Ind. Eng. Chem. Prod. Des. Deveop.*, **12**, 328(1973).
6. H. Strathmann, and K. Kock, *Desalintion*, **21**, 241(1977).
7. J. G. Wijmans and C. A. Smolders, "Synthetic membranes : Science, Engineering and Applications", P. M. Bungay, H. K. Lonsdale and M. N. de Pinho, Ed. D. Reidel Pub. Co. Dordrecht, Holland, 1986.
8. F. W. Altena and C. A. Smolders, *Macromolecules*, **15**, 1491(1982).
9. M. H. V. Mulder, J. O. Hendrikman, J. G. Wijmans, and C. A. Smolders, *J. Appl. Polym. Sci.*, **30**, 2805(1985).
10. J. G. Wijmans J. Kant, M. H. V. Mulder, and C. A. Smolders, *Polymer*, **26**, 1539(1985).
11. J. G. Wijmans, J. P. B. Baaij, and C. A. Smolders, *J. Memb. Sci.*, **14**, 263(1983).
12. L. Yilmaz and A. J. McHugh, *J. Memb. Sci.*, **28**, 287(1986).
13. L. Yilmaz and A. J. McHugh, *J. Appl. Polym. Sci.*, **31**, 997(1986).
14. J. D. Andradw, L. M. Smith and D. E. Gregonis, "Surface and Interfacial Aspects of Biomedical Polymers", Chap. 7, J. D. Andrade Ed., Plenum Press, N. Y.
15. H. Strathmann, K. Kock, P. Amar, and R. W. Baker, *Desalination*, **16**, 179(1975).